Mansoura Engineering Journal, (MEJ), Vol. 32, No. 3, September 2007. E. 26

Tracking High Performance of an Isolated PV-Diesel System Without Energy Storage

الحصول على أداء عال من منظومة مصفوفة خلايا شمسية مع مولد ديزل مستقلة بدون تخزين طاقة

A. Elmitwally, member, IEEE and M. Rashed, member, IEE
Elect. Eng. Dept.,
Mansoura University,
Mansoura, 35516, Egypt

ملخص

يقدم البحث طريقة مقترحة للتحكم فى منظومة قوى مستقلة تتكون من مصفوفة خلايا شمسية تشارك مولد ديزل فى تغذية حمل ثلاثى الأوجه بدون وجود وسط لتخزين الطاقة لخفض تكلفة المنظومة، و تهدف منظومة التحكم إلى استخلاص القدرة العظمى المتاحة من مصفوفة الخلايا الشمسية والحفاظ على قيمة جهد الحمل ثابتة وتعويض عدم الاتزان فى التيار بحيث يرى مولد الديزل حملا متزنا دائما وأيضا تثبيت التردد بتثبيت سرعة محرك الديزل عن طريق أسلوب مبتكر للتحكم فى العاكس الذى يربط الخلايا الشمسية بباقى المنظومة و استخدام حاكم سرعة يعتمد على شكل مطور لحاكمات المنطق المبهم، كما يتم دراسة أداء المنظومة تحت ظروف التحميل غير العادية و الوقوف على مشاكل التشغيل تحت الحمل المنخفض، و يقترح البحث منهجين لتعديل منظومة التحكم للتغلب على تلك المشاكل، الأول يعتمد على تعديل القيمة المرجعية لجهد وصلة التيار المستمر وفقا للحمل والثانى يبنى على تعديل الدائرة بإدخال مقطع تيار مستمر بين الخلايا و العاكس، وقد أظهرت النتائج المقارنة فاعلية كلا المنهجين بالحصول على أداء ممتاز فى جميع الظروف المحتملة للتشغيل.

Abstract

In this paper, a control scheme is proposed for three-phase isolated PV-diesel system without energy storage element. The scheme aims to: track maximum power from the PVA, regulate the load voltage, compensate the load unbalance viewed by the diesel generator, and to control the diesel engine speed. The first three tasks are achieved by controlling the PWM inverter interfacing the PV array to the system. The fourth is realized by a modified fuzzy logic controller of the diesel engine. The obstacles encountered on operating the system under certain probable loading conditions are addressed. Two strategies are proposed to adapt the control scheme to accommodate all loading scenarios maintaining excellent technical and economic performance. The system operation is investigated under a variety of conditions to prove the aptness of the proposed techniques.

1.Introduction

Application of hybrid PV-diesel systems has been widely recognized as a reliable, feasible and environment-friendly solution to supply power to remote locations. Usually, the system is isolated from the utility grid as it is difficult and often infeasible to extend lines and feeders to these remote areas. The system is typically sized such that the PV array (PVA) size is almost equal to the expected load power. The diesel driven generator (DDG) supplies the deficit in the PVA output power due to insolation fluctuations. The co-ordinated operation of the PV-DDG offers a chance to eliminate the need for energy storage device to improve the system economics. Also, the PVA is fully utilized via devoted control that guarantees maximum possible output power from the PVA to make maximum fuel savings of the DDG. Such PV-DDG system without energy storage (see Fig.1) works well if the load is around its normal level. The DDG supplies at least a minimum power share to the system

Accepted September 30, 2007

(works in the normal generation mode) and the used speed control mechanism can keep the speed around its rated value. Thus, the load voltage magnitude and frequency (both are functions of speed) are maintained within their specified limits.

However, partial failure of load equipment is probable in these systems that will reduce the load power needs. For classic operation strategies, if the available load capacity is less than the maximally tracked PVA output power for certain climatic conditions, there will be excessive power production. This is supplied to the DDG (the direction of power flow is reversed) and the DDG operates as a motor. Under this condition, the speed control mechanism will fail to keep the DDG speed within the accepted limits. The speed increases steeply within a fraction of second time to a dangerous level much larger than its rated value. The later out-of-control high speed can have two severe impacts. The first, it will cause drastically increasing voltage magnitude and frequency with abnormal and deleterious values. This, in one hand, detracts dramatically the voltage quality and hence the performance of the load equipment. On the other hand, it may damage the load equipment and/or the interface inverter resulting in unwanted financial loss. The second, it will greatly increase the tear and wear in the diesel engine that may initiate mechanical deterioration to the diesel engine [1-3]. This may shorten its life time leading to earlier replacement that forms another financial loss. Therefore, the applied control scheme should be flexible enough to accommodate this possible condition of operation. It must assure a secure and high -quality performance of the PV-diesel system under all conditions without a need to a costly storage medium or even to switch off the system. That is what is tackled in this paper.

In [1], the dynamic interaction between a wind turbine generator (WTG), a DDG and local load is analyzed. The condition of DDG motoring is manifested and its impact on voltage magnitude and frequency is discussed. In [2], the operation of a DDG integrated to a variable speed WTG is analyzed. A flywheel power smoothing medium is introduced to flatten the power output of the DDG. This aids to prevent the deterioration of DDG if it is operated under fluctuating power production and speed affected by the fluctuating output power of the WTG. The complexity of the control and high cost of the treatment system are apparent.

Many studies reported the operation and control of hybrid energy systems under normal operating conditions [3-7]. In [3], the development of a predictive artificial neural network (ANN)-based controller for the optimum operation of hybrid renewable energy-based water and power supply system is presented. The system consists of PVA, DDG, battery bank for energy storage and a reverse osmosis desalination unit. The ANN controller is designed to take decision on diesel generators ON/OFF status in order to 1) maintain a minimum loading level on the DDG under light load and high insolation levels, 2) maintain high efficiency of DDG, and 3)switch off DDG when not required based on predictive information. In [4], genetic algorithms are used for the optimum design and sizing of hybrid photovoltaic systems. In [5], a control scheme of inverters to operate a micro-grid and provide good power quality is presented and compared with both traditional power systems and with control of dc/dc power converters. However, the problem of operation and control of stand alone PV-diesel systems without energy storage medium under emergency conditions is not yet addressed adequately in literature.

In this paper, a control scheme is proposed for three-phase isolated PV-diesel system without energy storage element. The scheme aims to: track maximum power from the PVA, regulate the PCC voltage, compensate the load unbalance viewed by the DDG, and to control the DDG speed. The first three tasks are achieved by controlling the PWM inverter interfacing the PVA to the system. The fourth is realized by a modified fuzzy logic controller

(FLC) of the DDG. The obstacles encountered on operating the system under particular loading conditions are highlighted. Two strategies are proposed to adapt the control scheme to accommodate all loading scenarios maintaining excellent technical and economic performance. The system operation is investigated under a variety of conditions to validate the proposed techniques.

II. System Description

Fig.1 depicts a schematic of the system presented in this paper. It consists of a PVA and a diesel driven synchronous generator supplying a three-phase R-L load. PVA size is 70 kW peak with 100 modules in series and 15 modules in parallel. The PVA is coupled to the ac load bus via a three phase IGBT PWM voltage source inverter (VSI). The DDG is also sized at the full common load power of 80 kW. This is to be able to support the load even the sun is absent at night. The DDG has a minimum loading limit of 5% of its capacity. The system operation objective is to produce enough power to the load with symmetrical three phase voltages with constant magnitude and frequency (50Hz) for all operating conditions within the maximum allowed loading limit. Meanwhile, the DDG current must be balanced to avoid torque pulsation, vibrations and excessive heating in the machine. This is subject to that the PVA shares the maximum possible portion of the load, irrespective of the load level, to maximize the fuel savings of the diesel engine. The inverter is to be controlled to achieve maximum power tracking of the PVA, balance the three-phase current of the DDG and to regulate the load voltage. Hence, the need for the DDG automatic voltage regulator (AVR) is eliminated. The PVA and the DDG models are given in [8]-[10]. The characteristics of PVA is depicted in Fig.2 for insolation levels (λ) from 1000 W/m^2 at the top to 100 W/m^2 at the bottom in 100 W/m^2 step and at temperature (T) 25 C°. It is targeted to achieve Maximum Power Tracking (MPT) from the PVA. Therefore, the operating dc voltage of the PVA that will provide maximum output power (V^*_{dc}) has to be determined for given values of λ and T.V^*_{dc} will be considered as the setting value of the VSI dc bus voltage. Multivariable linear regression technique is used in this study to compute V^*_{dc} as expressed in (1), [8].

$$V^*_{dc} = a_1\sqrt{\lambda} + a_2 T + a_3 \quad (1)$$

where a_1, a_2 and a_3 are regression coefficients.

III. The Proposed Control Scheme

The proposed control strategy of the inverter is based on the synchronous reference frame (SRF) technique. The sensed three-phase load currents are converted into three components (i_d, i_q and i_0) in the rotating d-q-0 reference frame at a transformation angle θ [11]. θ is a time varying angle that represents the angular position of the reference frame. θ is tracked from the sensed three-phase DDG voltages using a phase locked loop PLL [11,12]. The VSI control scheme is composed of two loops as shown in Fig.3. They are described in the following subsections.

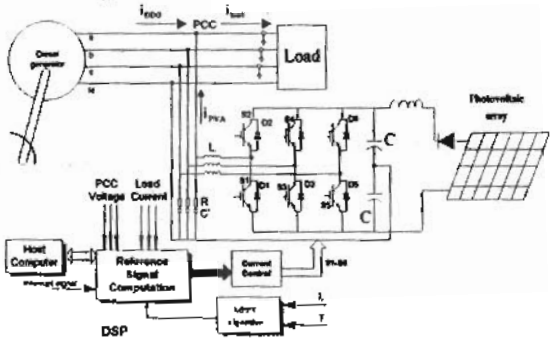

Fig.1 System block diagram

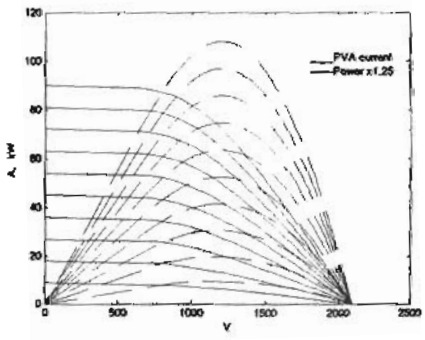

Fig. 2 I-V and power characteristics of PVA

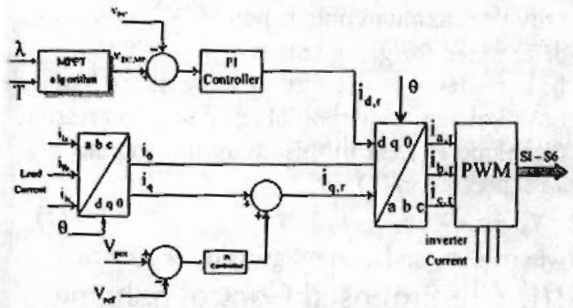

Fig.3. Schematic diagram of the VSI control system

A. The Maximum Power Tracking Loop

The actual dc bus voltage is sensed and compared to a dynamic setting point computed from (1). The difference ΔV_{dc} is processed in a PI controller to produce the d-axis reference current of the inverter ($i_{d,r}$).

B. Voltage control Loop

The inverter controller is supplemented by a loop dedicated to regulate the PCC voltage. This forces the inverter to inject adequate amount of fundamental reactive current with relevant sign into the power line. This current builds correcting voltage drop across the DDG series impedance X_L to regulate the PCC voltage. The peak PCC voltage (V_{PCC}) is compared to its reference value (V_{ref}). The error is processed in a PI controller to give a corrective fundamental reactive current $i_{q,VR}$ that is summed up with the q-axis current component of the load current.

C. PWM Control

The 2 loops described above are integrated as revealed in Fig.3. The net d, q and 0 components of the inverter reference currents, $i_{d,r}$, $i_{q,r}$ and i_0, are used to obtain the phases a, b and c reference currents of the inverter $i_{a,r}$, $i_{b,r}$ and $i_{c,r}$, through the inverse transformation [11]. The sampled error initiated by comparing the three-phase reference currents to actual inverter currents are processed in PI controllers to give the three phase voltage reference of the inverter $v_{a,r}$, $v_{b,r}$ and $v_{c,r}$. The PWM switching patterns of the inverter IGBT switches are obtained by comparing the reference voltage against a triangular carrier with 10kHz frequency.

D. Diesel Speed Control Sub-System

A FLC of speed is designed and used to stabilize the speed of the nonlinear DDG as given in [12]. The inputs to the FLC are the diesel engine speed error and the change of the error. The input/output membership functions are triangular shaped with 50% overlap. Each variable has 7 membership functions labeled from Negative Big NB to Positive Big PB. A rule base of 49 rules is selected to establish the fuzzy controller, [12]. With the use of Mamdani's implication and with defuzzification by a centroid method, the fuzzy controller provides the value ΔT^*_d [13]. The reference torque to the diesel engine governor T^*_{d-l} is computed from ΔT^*_d as [10]:

$$T^*_{d-l} = k_1 \Delta T^*_d + k_2 \int \Delta T^*_d dt \qquad (2)$$

where k_1 an k_2 are adjusted constants.
The estimated load torque T_l is given by:

$$T_l = \frac{1}{\omega_r} \sum_j \left(V_{L,j} + R_a i_{g,j} + L_a \frac{di_{g,j}}{dt} \right) i_{g,j} + B\omega_r \qquad (3)$$

where: j refers to the phases a, b and c, V_L is the load voltage (V), R_a is the generator armature resistance (Ω/phase), L_a is the generator armature inductance (H/phase), B is the friction coefficient of the DDG (Nm.s), i_g is the generator current (A) and ω_r is the diesel engine angular speed (rad/s). T_l is fed forward and added to T^*_{d-l} as an equivalent control signal to enhance the capability of the diesel engine to reject load disturbances [10]. The resultant output is the reference torque signal T^*_d to the governor of the diesel engine, which should be practically smooth at steady state. Fig.4 shows the speed control system of the diesel engine.

A full dynamic model of the system given in Fig.1 and its control scheme is constructed in Matlab/ Simulink environment. A list of the parameters used in simulation is provided in Table 1. The insolation level is 1000 W/m^2 and the temperature is 25 C^o.

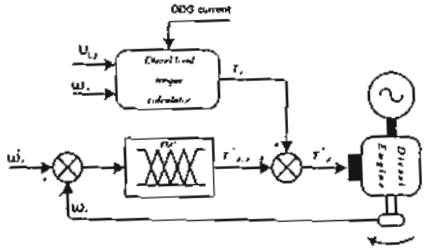

Fig.4 Speed control system of the diesel engine

A sudden drop of the load to 50% of its normal level at 0.6 s is considered. Figs. 5 and 6 depict the system performance. Fig.5a shows the PVA output power (the dotted), the load power (the solid) and the DDG output power (the dashed). It is noted that the PVA output power is held constant at its maximum level of 70 kW irrespective of the load reduction as dictated by the maximum power tracking control. Before load change, the DDG is generating about 8 kW. When the load drops at .6 s, the DDG takes the excessive power supplied by the PVA (negative value for DDG power) and operates in the motoring mode. This situation results in steeply accelerating the DDG rotor. As in Fig.5b, the speed is nearly held at its rated value (157 rad/s) before the sudden load change at .6 s where the speed starts to increase steadily. It reaches twice of its nominal value at 1.5 s. This causes similar increase in both magnitude and frequency of the DDG generated voltage. The frequency varies from 50Hz at .6 s to about 100 Hz at 1.5 s. Besides, the PCC peak phase voltage changes from 308 V (nominal) at .6 s to about 500 V at 1.5 s as shown in Fig. 5c. Fig. 6a reveals the waveform of phase a voltage at PCC. The steady increase in magnitude and frequency is noticed after the sudden load reduction at 0.6 s. Fig.6b depicts the phase a current of the VSI. Its magnitude increases after 0.6 s until it comes to its saturation limit at about .85 s forced by the saturation in the PI controllers used in the reference current computation of the VSI. The current increases as the VSI works to adjust the increasing PCC voltage by magnifying the drop across the series impedance of the DDG, X_L. Fig.6c illustrates the waveform of the phase a current of the DDG. The enlargement of the magnitude and frequency are marked after 0.6 s as the DDG absorbs higher power (during motoring) than the supplied before 0.6 s. The big increase in voltage magnitude and frequency due to the load reduction forms unwanted severe operating conditions to the load equipment as well as the VSI. This situation needs to be corrected by modifying the control strategy of the system, namely the maximum power tracking loop, as discussed in the following sections.

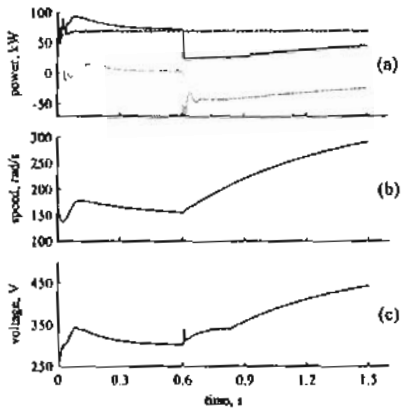

Fig.5 Performance for the basic control system

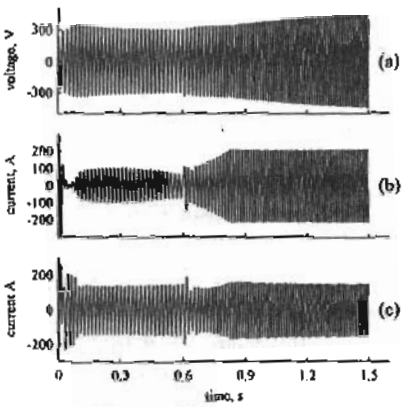

Fig.6 Waveforms of the basic control system

IV. Control Scheme Modifications

A. First strategy

It is based on two considerations. The first is that load must be fed by the PVA whenever possible to maximise the fuel savings of the

DDG. The second is that the dc bus voltage should not exceed a certain upper limit as it is not desired for the inverter switches. The modification scheme depends on varying the operation dc voltage of the PVA (V_{dc}) away from the maximum power dc voltage (V^*_{dc}) given in (1). If the load power is less than the maximum output power of the PVA, the V_{dc} is adjusted using the PVA characteristics given in Fig.2 such that the PVA outputs just the load power minus a fixed quantity (4 kW) equivalent to the lower limit production of the DDG. Thus, the output PVA power is reduced below the load power and no power is delivered to the DDG avoiding unwanted speed, voltage and frequency drastic increase. For a certain value of the PVA power less than the maximum power, there are two possible values of V_{dc} on the both sides of V^*_{dc} (see Fig.2). The higher one should be selected to ensure proper operation of the VSI. However, the required new V_{dc} of the PVA may be prohibitively large and can highly stress the inverter switches. So, the V_{dc} is set at un upper limit of 1600 V. This may render the PVA output power still higher than the load power that keeps the problem. To manage this situation, the difference between the PVA output power at 1600 V and the load power is dropped by disconnecting a number of the parallel modules of the PVA. The PVA is partitioned into 5 groups of parallel modules with 3 modules in each group. If V_{dc} is set at its upper limit, one or more groups is disconnected lowering the PVA output power below the load power and automatically V_{dc} is readjusted below its upper limit. If the load is increased above the maximum output power of the still-connected PVA groups, V_{dc} is lowered to V^*_{dc} to increase the PVA output power. If it does not suffice the load, one or more of the disconnected module groups is reconnected. This algorithm is shown diagrammatically in Fig.7.

B. Second strategy

It involves a circuitry modification in the system hardware, and then the overall control scheme is adapted accordingly. A dc boost chopper is incorporated as a link between the dc bus and the PVA. The operating dc voltage of the PVA, V_{dc}, is varied such that the output PVA power equals almost the load power as long as the load power is less or equal to the maximum output power of the PVA. Otherwise, V_{dc} is set at V^*_{dc}. The load power considered in this judgement is lowered by a fixed value (4 kW) that is corresponding to the lower loading limit of the DDG.

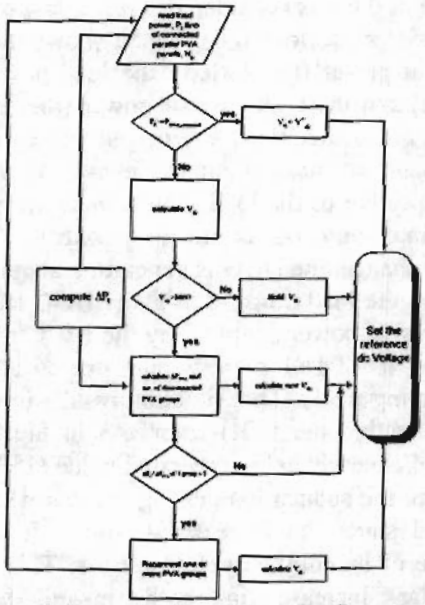

Fig.7 Schematic diagram of the first strategy

The desired V_{dc} is realised via the proper control of the dc chopper. The latter is current-controlled to set the required V_{dc} at its input. The dc bus voltage is maintained through the inverter control at a fixed value that is 1200 V. A prime step in the control algorithm is to estimate the operating PVA current (I_{PVA}) that corresponds to a certain amount of the required power. A large family of curves relating the PVA output power to its dc current at different insolation levels is established (see Fig.8) through the used PVA model. These curves are stored in a look-up table to speed up the response of the control algorithm. Since there are two values of I_{PVA} for any given value of

PVA power (from the PVA characteristics Fig.2), the higher of which is selected. This imposes lower V_{dc} than V^{*}_{dc} that is necessary for the proper operation of the dc chopper. This is because the dc chopper is a boost chopper which assumes that the dc voltage on its input (PVA side) is less than the dc voltage on its output (the dc bus side). The reference input current of the dc chopper ($I_{ch,ref}$) is determined from the look-up table for a certain load power and then compared to the actual input current. The error signal is processed in a PI controller to produce the PWM switching signals of the IGBT chopper switch. The scheme is illustrated diagrammatically in Fig.9.

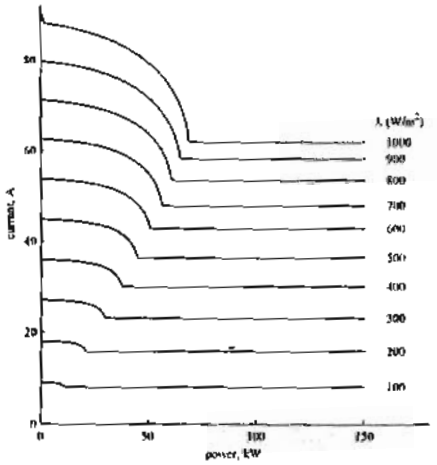

Fig.8 Current-power characteristics of the PVA

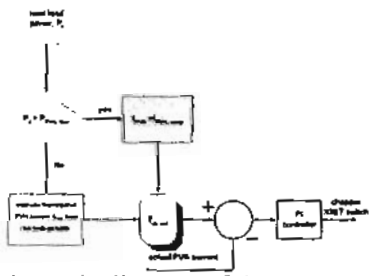

Fig.9 Schematic diagram of the second strategy

V. Performance of the system

Two dynamic models of the system with the two modified control schemes are constructed and simulated using the power system simulator (SimPower) in the MATLAB/SIMULINK environment. The two modifying control strategies discussed in section. IV are implemented as C^{++} S-functions in the system model [14]. A list of the system parameters considered in simulation is put in Table 1. The insolation level is 1000 W/m^2 and the temperature is 25 C°. The system is examined for achieving maximum power extraction of the PVA, DDG currents unbalance removal and PCC voltage regulation under extreme operating conditions. The performance of the two control modification schemes is evaluated.

Table I System parameters used in simulation

DDG side	Phase voltage: 220 V (rms), frequency: 50 Hz rated speed =157 rad/s X_a = 0.352 Ω/phase R_a = 0.062 Ω/phase
PVA side	Reactor, L_{dc} = 10 mH a_1 = 2.86, a_2 = -2.95 and a_3 = 1183.29
VSI	dc bus capacitor = 10000 μF, L_{inv} = 3 mH, switching frequency =10 kHz,
Load	active power = 80 kW, reactive power = 30 kVar

The system load changes suddenly at 0.6 s from the full balanced load of 80 kW to a light balanced load of only 27 kW as shown in Fig.9a. The system performance for the first strategy (section IV. A) is revealed in Figs. 9 and 10. Fig.9 reveals the following from top to bottom: a) the load power, b)the PVA power (the dotted) and the DDG power (the solid), c)the dc bus voltage, d) the DDG speed, and e)the number of still-connected parallel PVA modules (Np). The PVA output power gets down from 70 kW to 23 kW at o.6 s and the DDG power is reduced from 20 kW to about 4 kW (Fig.9 b) in response to the large step load reduction at 0.6s.

The controller changes the V_{dc} away from V^{*}_{dc} (1200 V) to the maximum permissible voltage

(1600 V) to reduce the PVA power (Fig 9c). Since the new dc voltage alone will make the PVA power still clearly higher than the load, which is unwanted, the controller disconnects some parallel modules of the PVA to work only with 5 parallel modules (one group) as in Fig.9e. This double action leads to tailor the PVA output to match this light load without disturbing excessive power. Hence the DDG is still operating in the generating mode with minimal output to maximize the fuel savings as desired. Its speed is maintained tightly around its reference (Fig. 9d). Fig.10 reveals the following from top to bottom: a) the three-phase VSI current waveforms, b) the three-phase DDG current waveforms, c)the amplitude of the voltage phasor (peak phase voltage), and d) the phase a voltage waveform at PCC. The three phase DDG currents are nearly sinusoidal and balanced (Fig.10b). Also, the PCC peak phase voltage is kept almost constant at its rated value (308 V) as shown in Fig. 10c. PCC phase voltage is clearly sinusoidal with fixed 50Hz frequency as desired (Fig.10d). This reflects the efficacy of the control scheme. The system performance for the second strategy (section IV. B) is depicted in Figs.11 and 12. Fig.11 reveals the following from top to bottom: a) the load power, b)the PVA power (the dotted) and the DDG power (the solid), c)the dc bus voltage, d) the DDG speed, and e) the amplitude of the voltage phasor (peak phase voltage). The PVA power is lowered to nearly match that of the load allowing a small power supplied by the DDG keeping it in generation mode (Fig.11b). V_{dc} and the DDG speed are kept at their references with very minor transients following the step reduction in the load, Fig.11c,d. The peak phase voltage is almost constant (Fig.11e). Fig.12 reveals the following from top to bottom: a) the three-phase VSI current waveforms, b) the three-phase DDG current waveforms, c)PVA current, and d) the phase a voltage waveform at PCC. The phase a voltage waveform is sinusoidal with fixed 50Hz frequency as required (Fig.12d). To achieve this, the controller varies the dc current of the PVA away from the maximum power dc current towards the high current region (less power) as in Fig.12c to adjust the PVA output to nearly that needed by the load avoiding DDG motoring and any unwanted violations in frequency and voltage.

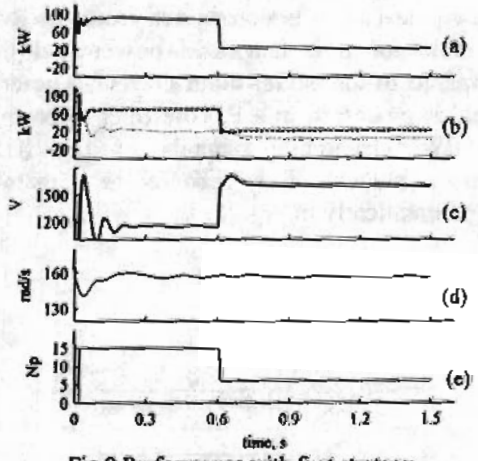

Fig.9 Performance with first strategy

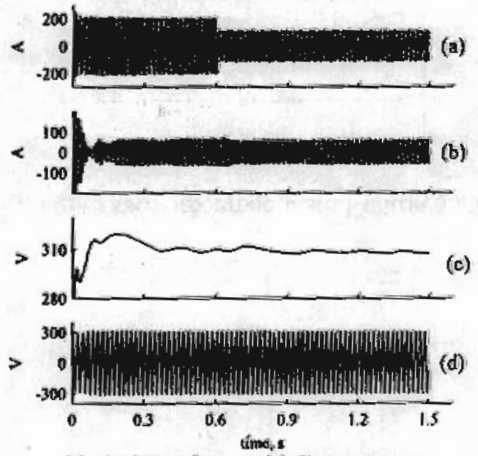

Fig.10 Waveforms with first strategy

C. Comparison

Fig.13 depicts a comparison of the performance of the two proposed strategies for the case of step reduction in the load discussed in section V.

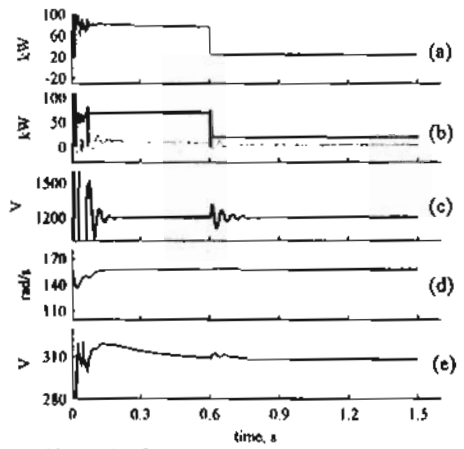

Fig.11 Performance with second strategy

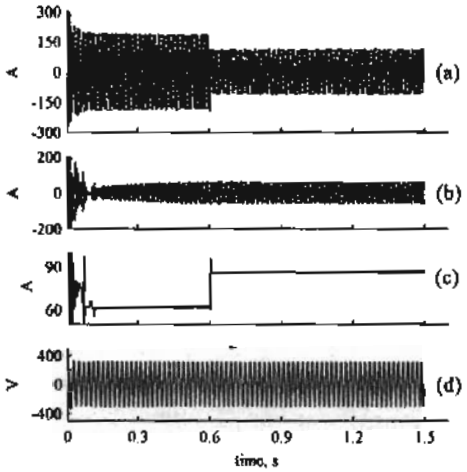

Fig.12 Waveforms with second strategy

Fig. 13a shows the DDG response for the first strategy in the dotted line and for the second strategy in the solid line. The performance specifications for speed control are given in Table 2 for both strategies. Fig. 13b shows the peak phase voltage at PCC for the first strategy in the dotted line and for the second strategy in the solid line. The performance specifications for voltage control are given in Table 3 for both strategies. It is remarked that the second strategy has a tangibly better performance in controlling the speed. Meanwhile, the both are fairly equal in regulating the PCC voltage. The cost of switches required to switch on/off the parallel modules of PVA for the first strategy is counterbalanced by the cost of the dc chopper involved in the second strategy. Hence, the second strategy is proved to be more advantageous.

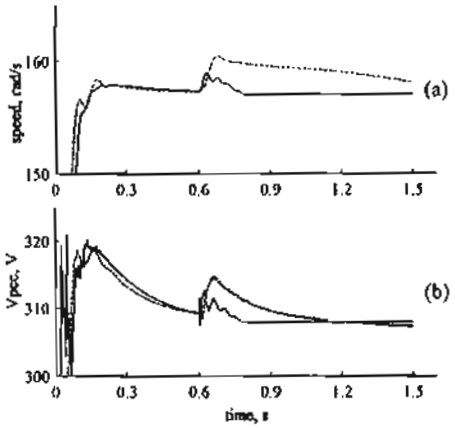

Fig.13 Comparison of the two strategies

Table 2 Performance comparison for speed

Strategy	Settling time (s)	Overshoot %	Mean error (rad/s)	Mean square error (rad/s)^2
First	>0.9	2.22	0.86	9.29
Second	0.26	1.27	-0.405	9.30

Table 3 Performance comparison for voltage

Strategy	Settling time (s)	Overshoot %	Mean error (V)	Mean square error (V)^2
First	0.32	2.27	1.23	216.5
Second	0.44	1.62	0.706	279

VI. Conclusion

A control scheme is proposed for three-phase isolated PV-diesel system without energy storage. The scheme aims to: track maximum power from the PVA, regulate the PCC voltage, compensate the load unbalance viewed by the DDG, and to control the DDG speed. The first three tasks are achieved by controlling the PWM inverter interfacing the PVA to the system. The fourth is accomplished by a modified fuzzy logic controller of the DDG. The problem of voltage magnitude and frequency escalation under particular loading conditions is focused. Therefore, two strategies are proposed to adapt the control scheme to accommodate all loading scenarios maintaining excellent technical and

economic performance. The first strategy depends on varying the dc bus voltage reference according to the load. The second involves a dc chopper between the PVA and the inverter. The both customize the PVA output power to just meet the load needs under high insolation and light loading. The main control system scored its intended performance objectives. The two proposed modifying strategies make the system operate successfully and up to the target under all conditions. The second strategy is noted to be slightly more apt.

VII. References

[1] Eduard Muljadi and H. Edward Mckenna, "Power Quality Issues in a Hybrid Power System," IEEE Transactions on Industry Applications, Vol. 38, No.3, 2002, pp.803-809.

[2] Cardenas, R.; Pena, R.; Clare, J.; Asher, G., "Power Smoothing In A Variable Speed Wind-Diesel System," IEEE Power Electronics Specialist Conference, 2003, PESC '03, 15-19 June, 2003, pp. 754 – 759.

[3] Ali Al-Alawia, Saleh M Al-Alawib and Sayed M Islam, "Predictive Control Of An Integrated PV-Diesel Water And Power Supply System Using An Artificial Neural Network," Renewable Energy Journal, Vol. 32, 2007, pp.1426–1439.

[4] Rodolfo Dufo-Lo´pez, Jose´ L. Bernal, "Design And Control Strategies Of PV-Diesel Systems Using Genetic Algorithms," Solar Energy Journal, vol.79, 2005, pp. 33–46.

[5] T.C. Green and M. Prodanovi´c, "Control Of Inverter-Based Micro-Grids," Electric Power Systems Research, EPSR-2401, 2007, in press.

[6] Thanaa F. El-Shatter, Mona N. Eskander and Mohsen T. El-Hagry, "Energy Flow And Management Of A Hybrid Wind/PV/Fuel Cell Generation System," Energy Conversion and Management, vol. 47, 2006, pp.1264–1280.

[7] Wakao, S.; Nakao, K.; "Reduction of Fuel Consumption in PV / Diesel Hybrid Power Generation System by Dynamic Programming Combined With Genetic Algorithm," Conference Record of the 2006 IEEE 4th World Conference on Photovoltaic Energy Conversion, Volume 2, May 2006, pp. 2335 – 2338.

[8] D. Canever, G.J.W. Dudgeon, S. Massucco, J. R. McDonald, and F. Silvestro, "Model Validation and Coordinated Operation of a Photovoltaic Array and a Diesel Power Plant for Distributed Generation," IEEE PES Summer Meeting, 2001, pp. 626-631.

[9] E.S. Abdin, A.M. Osheiba and M.M. Khater, "Modeling and Optimal Controllers Design for a Stand-Alone Photovoltaic-Diesel Generator Unit", IEEE Transaction on Energy Conversion, Vol. 14, No. 3, September 1999, pp. 560-565.

[10] D. J. McGowan, D. J. Morrow, and B. Fox, "Integrated Governor Control for a Diesel-Generating Set," IEEE Transactions on Energy Conversion , Vol. 21, No. 2, June 2006, pp. 476–483.

[11] G. D. Marques, "A Comparison of Active Power Filter Control Methods in Unbalanced and Non-Sinusoidal Conditions," Proceedings of IEEE IECON, 1998, pp.444-449.

[12] A. Elmitwally, S. Abdelkader and M. Elkateb, "Universal Power Quality Manager with a New Control Scheme," IEE Proceedings on Generation Transmission and Distribution (GTD), Vol. 147, No. 3, May 2000, pp. 190-196.

[13] Fuzzy Logic Toolbox, User's Guide Version 2, Mathworks, 1998.

[14] MATLAB/SIMULINK User's Manual, Version 3, Mathworks, 1999.